Journal of Engineering Science and Technology
Vol. 13, No. 11 (2018) 3500 - 3515

CHARACTERIZATION OF THREE DIMENSIONAL SCAFFOLDS FROM LOCAL CHITOSAN/ALGINATE/GEOTHERMAL SILICA FOR POTENTIAL TISSUE ENGINEERING APPLICATIONS

YUNI KUSUMASTUTI[1,2,*], MIME KOBAYASHI[3], FISKA YOHANA PURWANINGTYAS[1], MAZAYA NAJMINA[1], HIMAWAN TRI BAYU MURTI PETRUS[1], NUR ROFIQOH EVIANA PUTRI[1], BUDHIJANTO[1], MASAO TANIHARA[3]

[1]Chemical Engineering Department, Universitas Gadjah Mada,
Jl. Grafika No. 2, Kampus UGM, Yogyakarta 55281, Indonesia
[2]Bioresource Engineering Group, Universitas Gadjah Mada,
Jl. Grafika No. 2, Kampus UGM, Yogyakarta 55281, Indonesia
[3]Graduate School of Materials Science, Nara Institute of Science and Technology, 8916-5 Takayama, Ikoma, Nara 630-0192, Japan
*Corresponding author: yuni_kusumastuti@ugm.ac.id

Abstract

Biocomposite scaffolds can be used to repair bone damage caused by accident or illness. As natural polymers, chitosan and alginate have been widely used for biocomposite applications. However, chitosan-based biocomposites have low mechanical strength. In Indonesia, geothermal power plants produce silica sludge as industrial waste containing around 50% amorphous silica. In this study, geothermal silica was purified and incorporated into chitosan-based scaffolds via a lyophilized method. In addition to Fourier transform infrared spectroscopy analysis, physical properties such as gelation, swelling ratio, and mechanical strength were analysed to assess the effects of the geothermal silica. The presence of silica was found to decrease the swelling ability in the biocomposites and increase mechanical strength. The highest mechanical strength was achieved at composition ratio of chitosan:alginate:geothermal silica = 1:1:1. Scanning electron microscopy analysis confirmed that the silica addition resulted in larger interconnected pores in scaffolds, which help increase cell infiltration and nutrient absorption for cell growth. Larger pores may have contributed to the decrease in swelling ability of the biocomposites while silica contributed to stronger structure under wet condition. The biocompsites did not show any indication of cytotoxicity on mammalian cell culture systems. Results of this study shed light on the potential of industrial waste as raw materials for tissue engineering applications.

Keywords: Alginate, Chitosan, Geothermal silica, Scaffold.

1. Introduction

Bone has a crucial role in humans, giving the body shape (frame) and supporting motion and flexibility. Because of its role, bone often encounters damage caused by accidents. As people age, bone becomes more susceptible for fractions. In an aging society, demand for bone repair is expected to rise. Currently, the damage is mainly repaired by using autograft and allograft techniques [1]. However, such treatment has many drawbacks including limited replacement tissue, immune rejection and the possibility of disease transmission [1, 2]. With the development of three-dimensional (3D) scaffolding resembling conditions in the extracellular matrix (ECM), tissue engineering has attracted researchers' attention as an alternative method to overcome the limitations of conventional treatments. Through interactions between cells and scaffolds, newly differentiated cells replace the damaged cells resulting in the regeneration of a network system. After functioning as a place to promote cell growth and differentiation, scaffolds need to degrade not to compromise the regeneration process [3]. Henceforth, materials for scaffold fabrication must possess several characteristics such as an ability to bind cells, capability to support cell growth, biocompatibility, biodegradability and non-toxicity [4]**.** Among materials that have a great potential for 3D scaffolds are natural biopolymers.

As a maritime country, Indonesia has an abundant potential of marine resources, including shrimp and crab. These animals have a crustacean shell with low economic value, which tends to be wasted, although it contains 20-40% chitin. Chitin is a linear biopolymer with a high nitrogen content. One of chitin derivatives is chitosan, a polysaccharide compound mainly composed of glucosamine and N-acetyl glucosamine. [5]. Chitosan is regarded as a suitable choice for the formation of bone scaffolding because it is non-toxic, biocompatible and biodegradable [6] and has antibacterial properties [7].

With the existence of functional groups including amino and hydroxyl groups, chitosan is relatively easy to modify. For example, chitosan can be easily combined with anionic polysaccharides such as alginate through polyion complex (PIC) mechanism [8, 9**]**. Moreover, PIC scaffolds generally have greater stiffness than stand-alone polymers. In an aqueous environment, the chitosan-based PIC scaffold is more stable than the pure chitosan scaffold [10]. Chitosan can also be combined with inorganic materials that will enhance both the mechanical strength and biological properties of biocomposites.

Silica is a prospective inorganic material for grafting and has been used as a scaffold material [11, 12]. The addition of silica has shown both an increase in mechanical strength and promotion of cell proliferation [13]. In this study, we utilize geothermal silica waste as a source of silica for biomaterials. Silica scaling reduces power plant efficiency, and reduces 40% of plant productivity within a year [14]. Therefore, the silica scale formed by the precipitation of amorphous silica in pipelines of geothermal installations has to be dumped periodically. It is important to find a way to utilize this waste.

Taking into account that natural resources are abundantly available in Indonesia, this paper discusses the possibilities for the use of local chitosan/alginate/geothermal silica biocomposites as 3D scaffolds for tissue engineering.

2. Materials and Methods

2.1. Materials

A medical-grade local Indonesian chitosan powder (>90% degree of deacetylation, 10-500 cps viscosity, <1.5% ash content, <0.5% protein content) was obtained from PT Biotech Surindo (Cirebon, Indonesia). Geothermal silica was obtained from PT Geo Dipa Energi (Dieng, Indonesia). Low molecular weight chitosan and nanopowder silica (molecular weight 60.08 g/mol, diameter 10-20 nm, 99.5% purity based on trace metal) were purchased from Sigma-Aldrich (St. Louis, MO, USA). Dulbecco's Modified Eagle Medium (DMEM) was purchased from Nissui Pharmaceutical Co., Ltd. (Tokyo, Japan). Fetal Bovine Serum (FBS) was purchased from HyClone (Logan, UT, USA). Glacial acetic acid, sodium hydroxide, hydrochloric acid was purchased from Merck (Germany). Sodium alginate, ethanol and other materials were purchased from PT Brataco Chemika (Indonesia).

2.2. Purification of geothermal silica

Purification of silica was conducted using a set of three-neck flasks equipped with an electronic motor stirrer with a rotational speed of 400 rpm at constant temperature of 90°C. Dried and sifted silica mud as much as 20 grams, was dissolved in 1.5 N NaOH aqueous solution and stirred with an electric motor stirrer for 2 hours. The suspension was then filtered with a Büchner funnel. The filtrate was titrated with 2 N HCl aqueous solution to form a gel at pH 6. The gel was washed with distilled water repeatedly until the pH reached 7 [14].

2.3. Preparation of biocomposites

Biocomposites were prepared by dissolving chitosan powder in 60 mL of acetic acid solution 1% (v/v) until homogeneous mixture solution of chitosan 1% (w/v) was obtained. After that, sodium alginate 1% (w/v) was added. Silica 1% (w/v) was then added and stirred using a magnetic stirrer for 2 hours at room temperature to obtain a homogeneous mixture. Final biocomposites were obtained through freeze-drying [14]. Commercially available chitosan and alginate were used and the silica composition of the biocomposites was varied by adding different amount of either local chitosan or geothermal silica as listed in Table 1.

2.4. Characterization

The content of geothermal silica after the purification process was analysed by Energy Dispersive X-ray Spectroscopy (EDX; EDX-8000, Simadzu Co., Kyoto, Japan). The EDX machine was equipped with a 10 mm collimator and the analysis was carried out in vacuum using Al-U and C-Sc analytes. The functional groups of biocomposites were analysed by Fourier Transform Infrared (FTIR) spectroscopy (Shimadzu IR Prestige 21, Japan) in the range from 500 to 4500 cm^{-1} based on the KBr method with 2 scans and a resolution of 4 cm^{-1}. Lyophilized biocomposites were sputter-coated with gold (50 nm) using a VPS-020 quick coater (ULVAC Inc., Kanagawa, Japan) for morphology observation by Scanning Electron Microscopy (SEM; S-4800, Hitachi High-Technologies Corp., Tokyo, Japan) at an acceleration of 15 kV.

2.5. Mechanical properties

The scaffolds' tensile strength was investigated using a testing machine (Pearson Panke Equipment Ltd., UK) following the ASTM D638-02 standard test method. Young's modulus (E, Mpa) of lyophilized scaffolds (10 mm × 60 mm × 7 mm) composed of different composition ratios were calculated. The value of Young's modulus, which depends on the load measured by the tensile strength testing machine (F, N) and cross-sectional area of scaffold samples (A, m^2), was determined by using Eq. (1).

$$E = \frac{F}{A} \tag{1}$$

Table 1. Biocomposite variations.

No.	Composition (Chitosan: Alginate: Geothermal Silica)	Local Chitosan	Chitosan Sigma- Aldrich **low molecular weight*		
		Geo-thermal Silica (A)	Nano-silica Sigma- Aldrich (B)	Geo-Thermal Silica (C)	Nano-silica Sigma-Aldrich(D)
1	1:1:0	A1	B1	C1	D1
2	1:1:0.5	A2	B2	C2	D2
3	1:1:1	A3	B3	C3	D3
4	1:1:1.5	A4	B4	C4	D4
5	1:1:2	A5	B5	C5	D5

2.6. Swelling study

In order to determine the amount of fluid absorbed into the biocomposites, a swelling study was performed. After lyophilized biocomposites were cut into a cylinder shape of approximately 7 mm height and 7.5 mm in diameter, the dry weight of the scaffolds was recorded as (W_D). They were then inundated in Phosphate Buffered Saline (PBS) utilizing a variety of drenching times: 1, 2 and 3 hour(s). The weight of the wet scaffolds was recorded as (W_W). The swelling proportion (S_R) was calculated with Eq. (2). [15]

$$S_R = \frac{W_w - W_D}{W_D} \tag{2}$$

2.7. Biodegradability Study

Scaffold degradation was studied by total immersion of the scaffolds into PBS for a certain period (4, 8, 12, 16 and 20 days) at 37°C. To maintain constant pH, the PBS was changed every day. After incubation, the scaffolds were taken out carefully and lyophilized by freeze drying. The weights of the initial lyophilized scaffolds (W_D) and the remaining scaffolds (W_r) were measured. Weight loss percentage or degradation percentage was calculated by the following equation [16].

$$Degradation\ percentage\ (\%) = \frac{W_D - W_r}{W_r} x100\% \tag{3}$$

Constant degradation rate (k) and order of reaction order (n) for degradation modelling were determined by the MATLAB® software (The MathWorks, Inc., Natic, MA, USA).

2.8. Biocompatibility study

The biocompatibility of chitosan-based biocomposites was assessed using the WST-8 assay. Lyophilized biocomposites were cut into approximately 12 mm^3, then put into a 24-well plate (Nunc, Denmark), and soaked in 75% ethanol for 15 min twice for sterilization. A collagen sponge (SpongeCol® 4 mm diameter, Advance BioMatrix, Carlsbad, CA, USA) was used as a 3D control and treated in the same manner. The scaffolds were dried under reduced pressure overnight. Prior to use, they were equilibrated in the Dulbecco's Modified Eagle Medium (DMEM) without Fetal Bovine Serum (FBS) for 4 hr. HeLa cells with a density of 1×10^4 cells/well with 1 mL/well DMEM supplemented with 10% FBS were seeded and incubated at 37 °C under 5% CO_2 conditions. Cells cultured without any scaffold were used as a 2D control. After incubation for 1, 3, or 7 days, 100 µL of WST-8 assay reagent (Dojindo, Kumamoto, Japan) was added into each well and incubated for 1 to 7 hours at 37 °C. The absorbance at a wavelength of 450 nm representing the number of viable cells was measured using a 96-well plate reader (Spectra Fluor Plus TECAN; Switzerland) after 100 µL each of the medium/solution was transferred to a 96-well plate (Nunc, Denmark). All experiments were conducted in triplicate.

2.9. Statistical analysis

Data represent mean ± standard deviation (SD) with triplicated experiments. The statistical analysis was performed using a one-way analysis of variance (ANOVA) to show significant differences with Tukey's post hoc test. *p* values less than 0.05 showed significant difference.

3. Results and Discussion

3.1. Geothermal silica characterization

Geothermal silica from PT. Geodipa Energy with ±50% silica content was purified by alkaline extraction. Atomic composition of the purified geothermal silica was analysed by Energy Dispersive X-ray Spectroscopy (EDX), with results shown in Fig. 1. The types of element present in the sample are represented by its energy in keV as shown on the horizontal axis. The number of X-Rays detected in the analysis is shown on the vertical axis with the intensity (cps) which was used to calculate the percentage of elements in the sample. The chemical composition of the purified sample is shown in Table 2. Although traces of impurities such as aluminium, sulphur, iron, calcium, and copper were detected, the purity of the obtained silica was nearly 98%.

Table 2. Atomic distribution of purified geothermal silica.

Component	Content % wt	Content (oxide form) % wt
Si	97.78	97.26
Al	1.18	2.06
S	0.67	0.31
Fe	0.18	0.24
Ca	0.16	0.11
Cu	0.03	0.02

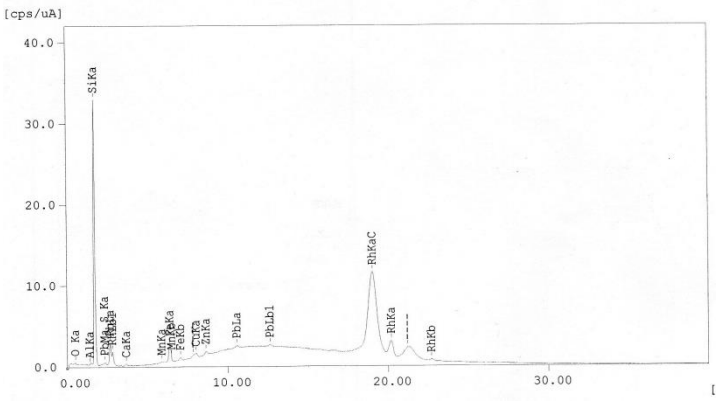

Fig. 1. EDX spectrum.

3.2. Chitosan/alginate/silica biocomposites

For tissue engineering application, purified silica was used to fabricate scaffolds. A different ratio of silica was mixed with chitosan and alginate to fabricate biocomposits as shown in Table 1. The effect of silica addition into chitosan/alginate biocomposites was first analysed by Scanning Electron Microscopy (SEM). The surface morphologies of the biocomposites are shown in Fig. 2. All biocomposites showed porous morphology, and blending of silica affected their structure. Larger interconnected pores in silica-containing biocomposites were observed most clearly when comparing A1 with A3, B1 with B3, and C1 with C3 in Fig. 2.

The SEM results indicate that the more silica content, the more interconnected pores. These interconnected pores are necessary to support cell attachment, cell infiltration, and tissue growth in the scaffolds [17]. Porous structures initially form through both nucleation and crystal growth during ice crystallization [18]. In addition to the nucleation, which affects the porous structure, the subsequent growth of ice crystals is also influenced by the solidification temperature [18]. With the increase of silica content, both the nucleation and growth of ice crystal may have changed. The formation of the condensed silica network might have disrupted the ice crystallization leading to morphology change [19].

Meanwhile, the use of geothermal silica and commercial silica did not produce a significant difference. Both silica gave good results in pore formation and similar pore-size range.

3.3. Tensile properties

Mechanical strength is another important factor for tissue engineering scaffolds. The result of the mechanical testing of the biocomposite scaffolds is shown in Fig. 3, representing the tensile properties. As expected, the addition of silica demonstrated higher Young's modulus values. Young's modulus values of silica incorporated chitosan/alginate with mass ratio of chitosan/alginate/silica = 1:1:1 with purified geothermal silica (A3) was significantly higher than that of chitosan/alginate biocomposite without silica (A1). Similarly, the nano-silica

incorporated scaffold with mass ratio of chitosan/alginate/silica = 1:1:1.5 (D4) was significantly higher than that of chitosan/alginate biocomposite without silica (D1). However, the composite with higher silica content represented with chitosan/alginate/silica = 1:1:2 (A5, D5) showed significantly lower Young's modulus compared to the chitosan/alginate/silica with ratio 1:1:1 (Fig. 3). The addition of silica at a certain ratio made the scaffold more brittle. This is due to the nature of silica itself, which is brittle and stiff [20]. The lower mechanical properties of the scaffolds might have also affected by uneven distribution of silica contents as shown in Fig. 4, resulting in non-uniform stress distribution [21].

Furthermore, the Young's modulus values of local chitosan/alginate/geothermal silica (sample A series) were lower than that of commercial chitosan/ alginate/ commercial silica (sample D series) in all ratios tested. This could be explained by the higher density of geothermal silica compared with commercial silica which might have affected inhomogeneous mixing of geothermal silica into the mixture. In addition, geothermal silica and commercial silica did not show any difference when incorporated into biocomposites, as indicated by the Young's modulus as shown in Fig. 5 (Compare A3 and B3; C3 and D3).

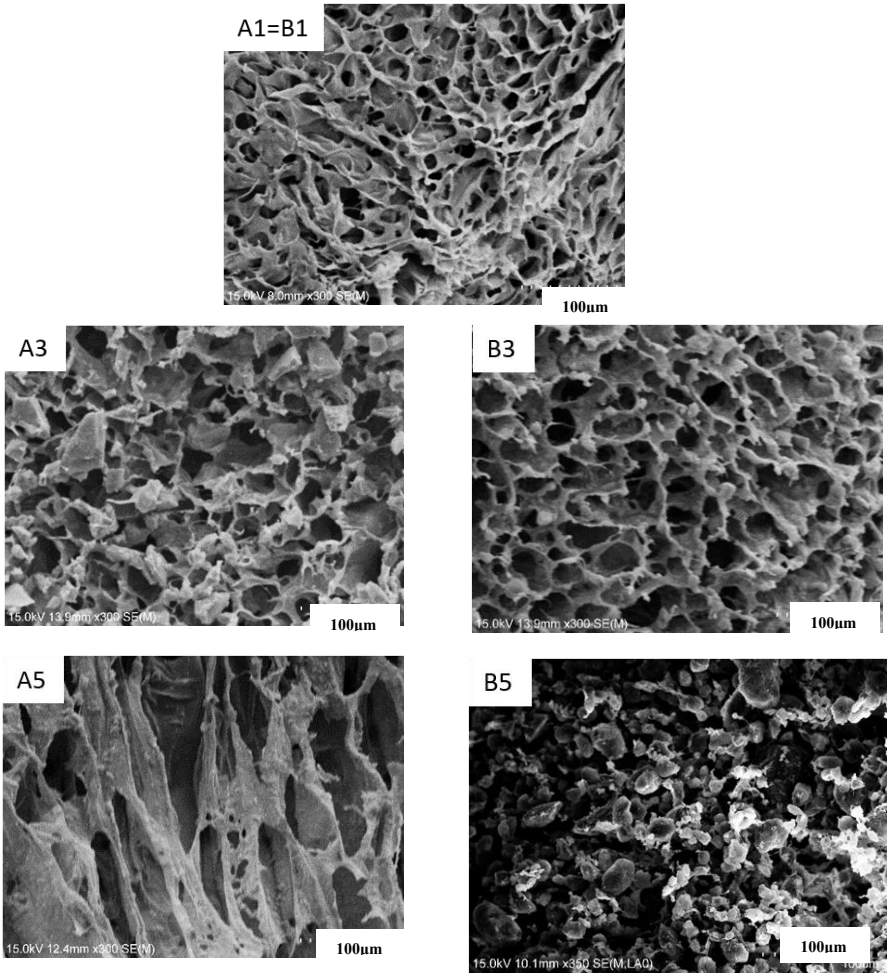

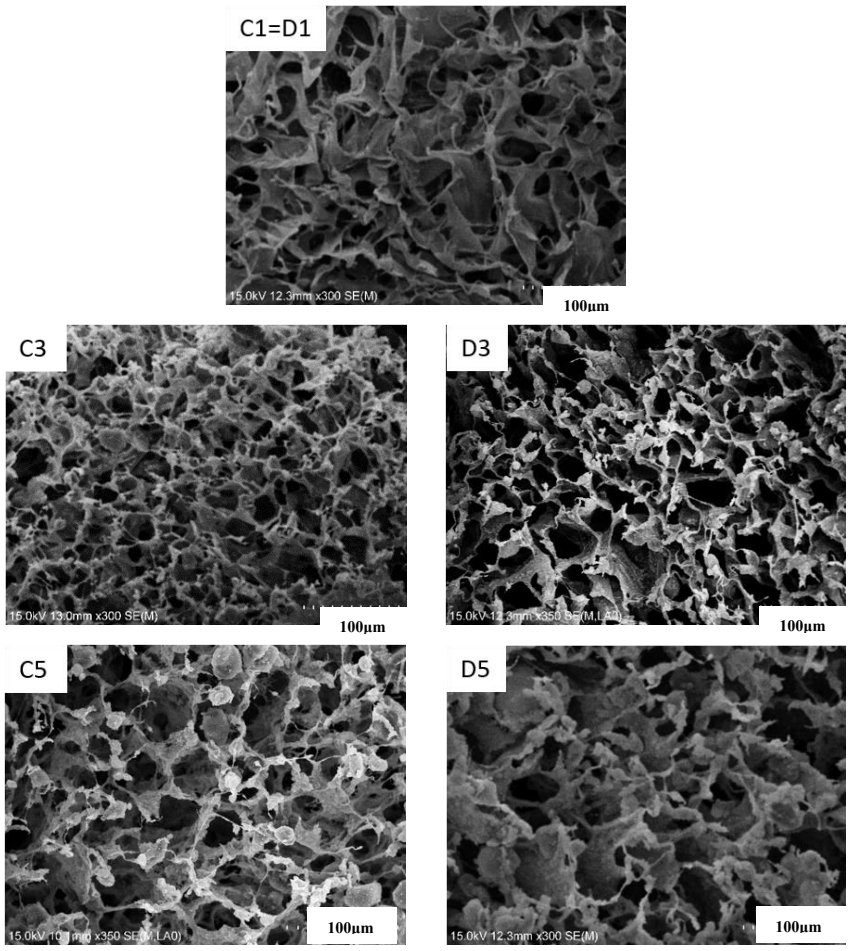

Fig. 2. SEM images of the lyophilized biocomposites.

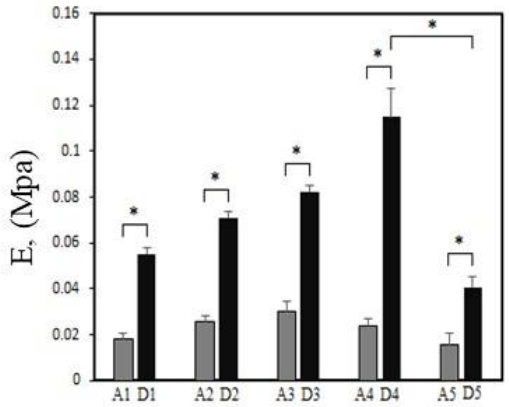

Fig. 3. The Young's modulus of the biocomposites (* represents p <0.05).

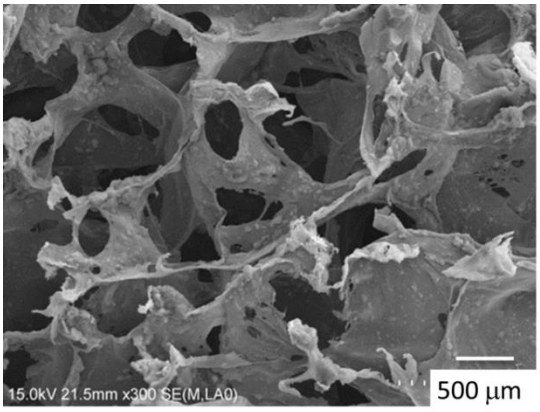

Fig. 4. Distribution of silica particles in a biocomposite (A3).

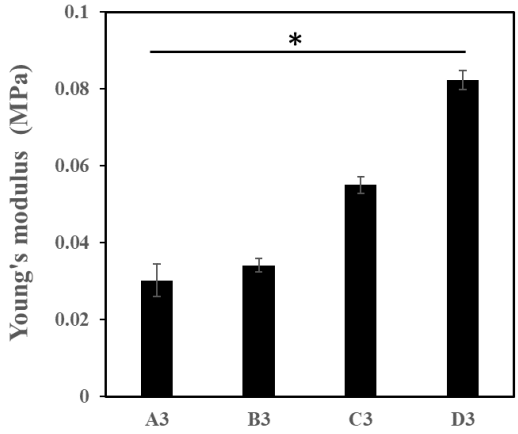

Fig. 5. Effects of geothermal silica or nano-silica addition on the Young's modulus of biocomposites. (* represents p <0.05).

3.4. FTIR analysis

Molecular interactions between biocomposite components were studied by Fourier Transform Infrared Spectroscopy (FTIR). As shown in Fig. 6**,** the spectrum of chitosan showed peaks of 1647 cm^{-1} of amide I and 1600 cm^{-1} of amide II. The result is similar with previous research studies [17]. Double peaks in the amide are caused by partial deacetylation of chitin [9]. The stretching vibration of OH and NH groups in chitosan is observed between 3200-3600 cm^{-1} [22].

Alginate commonly exhibits transmittance spectra of hydroxyl, ether, and carboxylic groups [23]. The spectral region around 1621cm^{-1} and ±1400 cm^{-1} are assigned to the asymmetric and symmetric stretching of -COO^-[24]. The -OH group appears as a broad peak between 3200-3600 cm^{-1} [25]. The band at approximately 2900 cm^{-1} is attributed to the stretching vibration of aliphatic C-H [26].

The peak at 1097 cm^{-1} is assigned to the asymmetric vibration of Si-O-Si in silica [27]. The peak of 3446 cm^{-1} shows the presence of -OH groups on the surface of $nSiO_2$ [9].

The interaction between chitosan and alginate leads to the band shift of amine group from 1647 cm^{-1} to 1632 cm^{-1} in chitosan/alginate biocomposites. A peak shift also occurred from 1600 cm^{-1} to 1561 cm^{-1} due to the interaction between carbonyl groups in chitosan and Si-OH groups of silica.

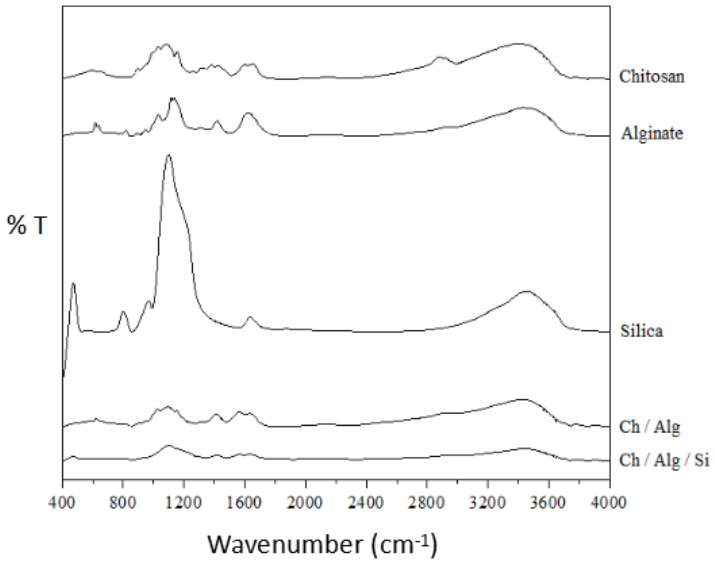

Fig. 6. FTIR spectra of pure components, biocomposites of chitosan/ alginate (Ch/Alg; A1), and chitosan/alginate/silica (Ch/Alg/Si; A3).

3.5. Swelling ratio

The ability of biocomposites to swell and absorb body fluid, transfer nutrients and metabolites inside the scaffolds plays an important role for cell proliferation [28]. First, biocomposites based on local chitosan were immersed in Phosphate-Buffered Saline (PBS) at room temperature to identify the maximum capacity of liquid uptake into the biocomposites. Figure 7 shows that the swelling ratio does not significantly change during 1- to 3-hour incubation periods. Based on this result, the same incubation period was used to investigate the swelling ratio of all biocomposites listed in Table 1 as shown in Fig. 8. The results indicate that by increasing the amount of silica content, the swelling ratio tends to decrease. Increasing the inorganic content might have induced stronger bonding between the organic and inorganic compounds, thus decreasing the hydrophilic chitosan content resulting in a decreased water sorption [29, 30]. The slower relaxation of the polymer chain caused by stronger organic-inorganic compound bonding may have also influenced the decrease in swelling ratio as described previously [17]. To be considered as a good candidate as a scaffold, not only the high swelling ratio should be achieved, but also the mechanical properties should be in an appropriate range. Proper ratio should be used to fulfil both parameters, depending on the specific purpose of the scaffolds.

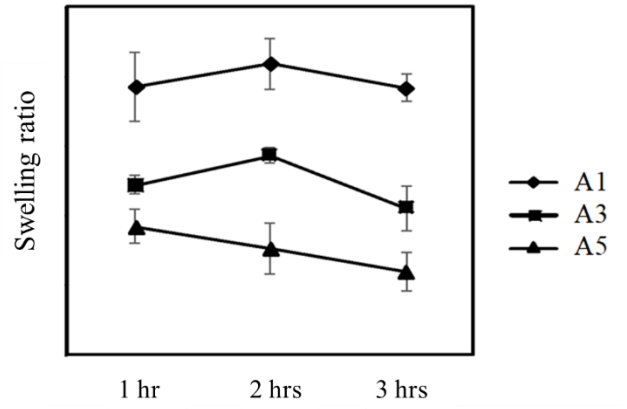

Fig. 7. Swelling ratio of biocomposites based on local chitosan after immersion in PBS for different periods.

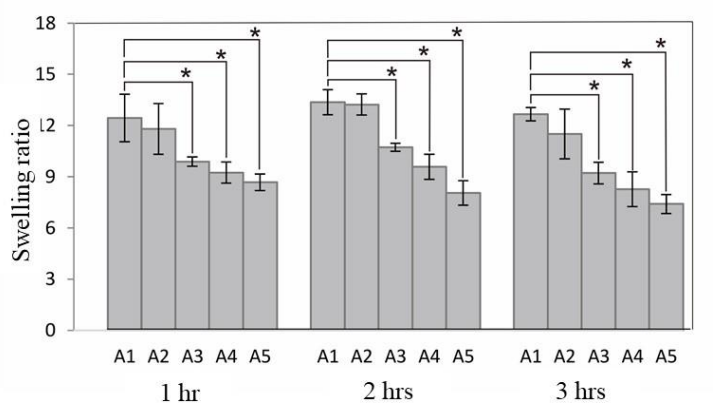

(a) Swelling ratio of biocomposites based on Local Chitosan/Geo-Thermal Silica.

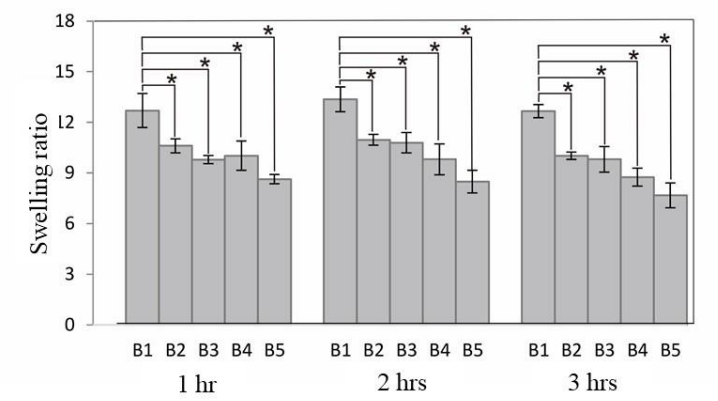

(b) Swelling ratio of biocomposites based on local chitosan/Nanosilica Sigma-Aldrich.

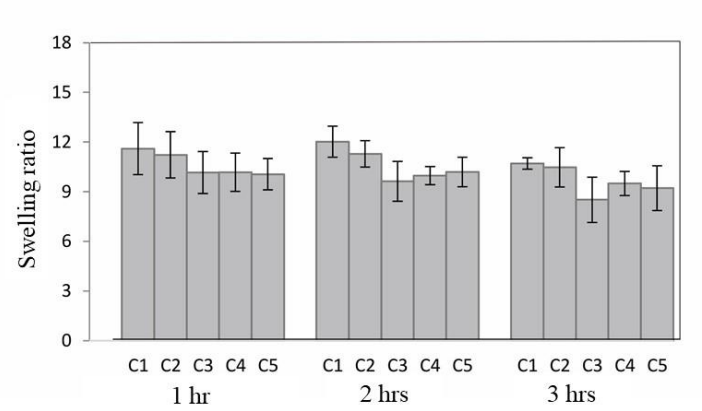

(c) Swelling ratio of biocomposites based on chitosan Sigma-Aldrich/Geo-Thermal Silica.

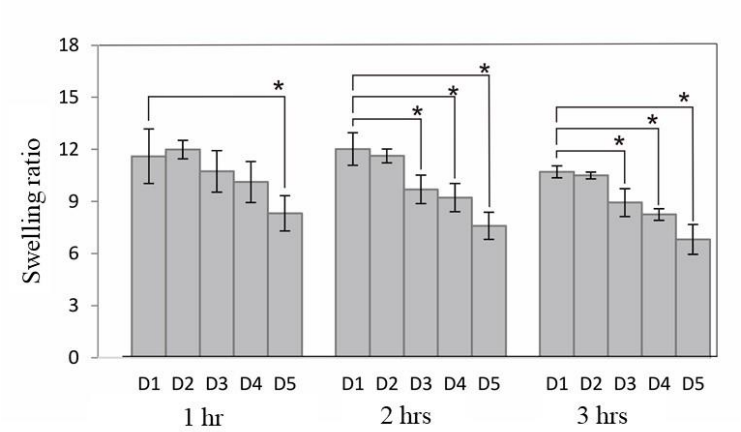

(d) Swelling ratio of biocomposites based on Chitosan Sigma-Aldrich/Nanosilica Sigma-Aldrich.

Fig. 8. Incorporation of silica decrease swelling ratio of the biocomposites (* represents p <0.05).

3.6. Biodegradability study

The scaffold degradation is also considered an important parameter in tissue engineering applications. The addition of geothermal silica into biocomposites, tends to increase the degradation rate of resulting scaffolds as shown in Fig. 9. The degradation rate constant (k^{-1}) was in the range of 0.02 - 0.06 day^{-1}. These trends are similar to a previous study [17]. The multiple crosslinking of alginate with Ca^{2+} and chitosan is affected by the addition of silica, thus showing a tendency to increase the degradation rate of scaffolds [17].

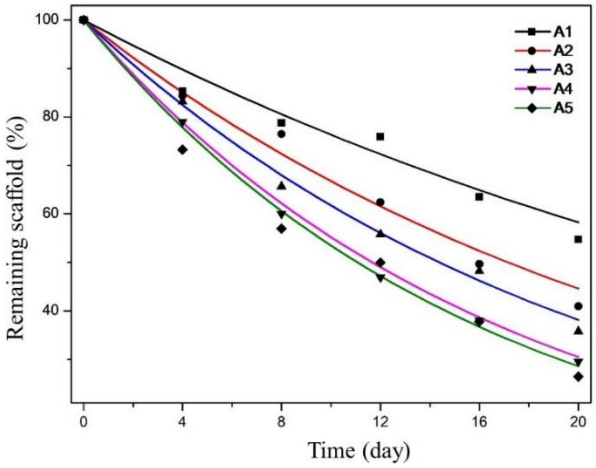

Fig. 9. Biodegradability study of biocomposites.

3.7. Biocompatibility study

The biocompatibilities of chitosan-based biocomposites were assessed by cell proliferation assays using WST-8 and HeLa cells with a cell culture period of 1, 3 and 7 days. After incubation for 7 days, no toxicity was observed for cells cultured in A1, A3, B3, C1, C3, and D3, as determined by cell survival rates, shown in Fig. 10. The proliferation of HeLa cells on local chitosan/alginate (A1) was not significantly different compared to the biocomposites from commercial chitosan/alginate (C1). Addition of geothermal silica into both local chitosan/alginate and commercial chitosan/alginate also showed no cytotoxicity. This result is similar to previous research conducted by Kavya, et.al, 2013, in which it is said that the incorporation of silica increases cell proliferation [23].

These results show that local chitosan and geothermal silica biocomposites are biocompatible and non-toxic for HeLa cells and promising to be suitable as scaffolds in tissue engineering applications.

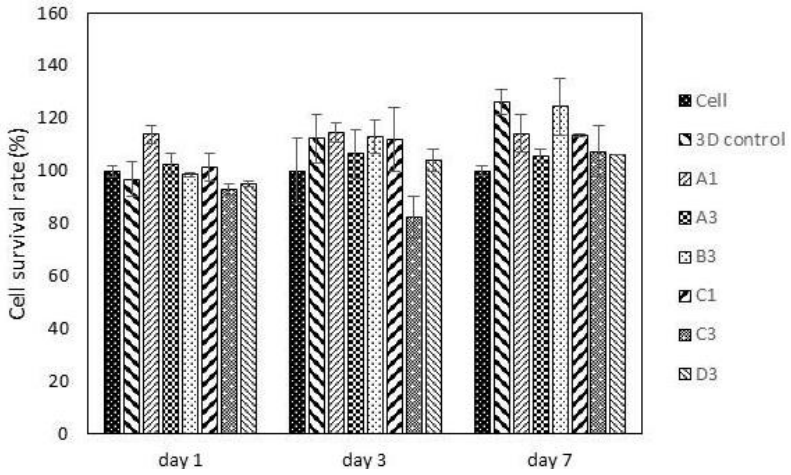

Fig. 10. *In vitro* biocompatibility analysis of the biocomposite scaffolds.

4. Conclusions

Chitosan/alginate/silica biocomposites using both locally and commercially produced components were analysed for the prospect of their utilization as scaffolds in tissue engineering. Geothermal silica is expected to improve the mechanical properties of scaffolds wherein the highest Young's modulus value was achieved at a composition ratio of chitosan:alginate:geothermal silica = 1:1:1. From cytotoxicity testing, the biocomposites using local components showed no significant hindrance compared with the ones using commercially obtained components. In silica-containing biocomposites, HeLa cells proliferated without any indication of cytoxicity compared to a collagen scaffold as a 3D control. These results suggest that local chitosan and geothermal silica biocomposites are biocompatible and promising scaffolds for tissue engineering applications.

Acknowledgment

The authors acknowledge the financial support from The Global Collaboration Program of Nara Institute of Science and Technology sponsored by Ministry of Education, Culture, Sports, Science, and Technology, Japan. English proofreading by Dr. Leigh McDowell is also acknowledged.

Nomenclatures

A	Cross-sectional area, m^2
E	Young's modulus, Mpa
F	Load, N
S_R	Swelling proportion
W_D	Dry weight, mg
W_W	Wet weight, mg

Abbreviations

3D	Three-dimensional
DMEM	Dulbecco's Modified Eagle Medium
ECM	Extracellular Matrix
EDX	Energy Dispersive X-ray Spectroscopy
FBS	Fetal Bovine Serum
FTIR	Fourier Transform Infrared Spectroscopy
PBS	Phosphate Buffered Saline
PIC	Polyion Complex
SD	Standard Deviation
SEM	Scanning Electron Microscopy

References

1. Venkatesan, J.; Bhatnagar, I.; Manivasagan, P.; Kang, K.H.; and Kim S.K. (2015). Alginate composites for bone tissue engineering: A review. *International Journal of Biological Macromolecules*, 72, 269-281.
2. Allison, D.C.; McIntyre, J.A.; Ferro, A.; Brien, E.; and Menendez, L.R. (2013). Bone grafting alternatives for cavitary defects in children. *Current Orthopaedic Practice*, 24(3), 267-279.

3. Loh, Q.L.; and Choong C. (2013). Three-dimensional scaffolds for tissue engineering applications: role of porosity and pore size. *Tissue Engineering Part B: Reviews*, 19(6), 485-502.
4. Bružauskaitė, I.; Bironaitė, D.; Bagdonas, E.; and Bernotienė, E. (2016). Scaffolds and cells for tissue regeneration: different scaffold pore sizes-different cell effects. *Cytotechnology*, 68(3), 355-369.
5. Medvecky, L. (2012). Microstructure and properties of polyhydroxybutyrate-chitosan-nanohydroxyapatite composite scaffolds. *The Scientific World Journal*, 2012(3), 537973.
6. Chen, Y.L.; Lee, H.P.; Chan, H.Y.; Sung, L.Y.; Chen, H.C.; and Hu, Y.C. (2007). Composite chondroitin-6-sulfate/dermatan sulfate/chitosan scaffolds for cartilage tissue engineering. *Biomaterials*, 28(14), 2294-2305.
7. Croisier, F.; and Jérôme, C. (2013). Chitosan-based biomaterials for tissue engineering. *European Polymer Journal*, 49(4), 780-792.
8. Kusumastuti, Y.; Putri, N.R.E.; and Dary, A.R. (2016). Electrospinning optimization and characterization of chitosan/alginate/polyvinyl alcohol nanofibers. *AIP Conference Proceedings*, 1755(1), 150007.
9. Kusumastuti, Y.; Shibasaki, Y.; Hirohara, S.; Kobayashi, M.; Terada, K.; Ando, T.; and Tanihara, M. (2017). Encapsulation of rat bone marrow stromal cells using a poly-ion complex gel of chitosan and succinylated poly(Pro-Hyp-Gly). *Journal of Tissue Engineering and Regenerative Medicine*, 11(3), 869-876.
10. Li, Z.; Ramay, H.R.; Hauch, K.D.; Xiao, D.; and Zhang, M. (2005). Chitosan-alginate hybrid scaffolds for bone tissue engineering. *Biomaterials*, 26(18), 3919-3928.
11. Schloβmacher, U.; Schröder, H.C.; Wang, X.; Feng, Q.; Diehl-Seifert, B.; Neumann, S.; Trautwein, A.; and Müller, W.E.G. (2013) Alginate-silica composite hydrogel as a potential morphogenetically active scaffold for three-dimensional tissue engineering. *RSC Advances*, 3, 11185-11194.
12. Lei, B.; Shin, K.; Noh, D.; Jo, I.; Koh, Y.; Choi, W.; and Kim, H. (2012). Nanofibrous gelatin-silica hybrid scaffolds mimicking the native extracellular matrix (ECM) using thermally induced phase separation. *Journal of Materials Chemistry*, 22(28), 14133-14140.
13. Fielding, G.A.; Bandyopadhyay, A.; and Bose, S. (2012). Effects of silica and zinc oxide doping on mechanical and biological properties of 3D printed tricalcium phosphate tissue engineering scaffolds. *Dental Materials*, 28(2), 113-122.
14. Kusumastuti, Y.; Petrus, H.T.B.M.; Yohana, F.; Buwono, A.T.; and Zaqina, R.B. (2017). Synthesis and characterization of biocomposites based on chitosan and geothermal silica. *AIP Conference Proceedings*, 1823(1), 020127.
15. Kucinska-Lipka, J.; Marzec, M.; Gubanska, I.; and Janik, H. (2017). Porosity and swelling properties of novel polyurethane-ascorbic acid scaffolds prepared by different procedures for potential use in bone tissue engineering. *Journal of Elastomers & Plastics*, 49(5), 440-456.
16. Díaz, E.; Sandonis, I.; and Valle, M.B. (2014). In vitro degradation of poly(caprolactone)/nHA composites. *Journal of Nanomaterials*, 2014, Article ID 802435, 8 Pages.
17. Sowjanya, J.A.; Singh, J.; Mohit, T.; Sarvanan, S.; Moorthi, A.; Srinivasan, N.; and Selvamurugan, N. (2013) Biocomposite scaffolds containing

chitosan/alginate/nano-silica for bone tissue engineering. *Colloids and Surfaces B: Biointerfaces*, 109, 294-300.

18. Pawelec, K.M.; Husmann, A.; Best, S.M.; and Cameron, R.E. (2014). A design protocol for tailoring ice-templated scaffold structure. *Journal of the Royal Society Interface*, 11(92), 20130958.
19. Wang, D.; Romer, F.; Connell, L.; Walter, C.; Saiz, E.; Yue, S.; Lee, P.D.; McPhail, D.S.; Hanna, J.V.; and Jones, J.R. (2015). Highly flexible silica/chitosan hybrid scaffolds with oriented pores for tissue regeneration. *Journal of Materials Chemistry B*, 3(38), 7560-7576.
20. Lemos, E.M.F.; Patrício, P.S.O.; and Pereira, M.M. (2016). 3D nanocomposite chitosan/bioactive glass scaffolds obtained using two different routes: an evaluation of the porous structure and mechanical properties. *Química Nova*, 39(4), 462-466.
21. Poh, P.S.P.; Bartnikowski, M.; Klein, T.J.; Kirby, G.T.S.; and Woodruff, M.A. (2015). Polycaprolactone-based scaffolds fabricated using fused deposition modelling or melt extrusioin techniques for bone tissue engineering. in *Biointerfaces: Where material meets biology*, *RSC Smart Materials*, 221-256.
22. Soliman, E.A.; El-Kousy, S.M.; Abd-Elbary, H.M.; and Abou-zeid, A.R. (2013). Low molecular weight chitosan-based Schiff bases: synthesis, characterization and antibacterial activity. *American Journal of Food Technology*, 8(1), 17-30.
23. Daemi, H.; and Barikani, M. (2012). Synthesis and characterization of calcium alginate nanoparticles, sodium homopolymannuronate salt and its calcium nanoparticles. *Scientia Iranica*, 19(6), 2023-2028.
24. Wang, Y.; Wang, X.; Shi, J.; Zhu, R.; Zhang, J.; Zhang, Z.; Ma, D.; Hou, Y.; Lin, F.; Yang, J.; and Mizuno, M. (2016). A biomimetic silk fibroin/sodium alginate composite scaffold for soft tissue engineering. *Scientific Reports*, 6, 39477.
25. Bajpai, S.K.; Bajpai, M.; and Shah, F.F. (2016). Alginate dialdehyde (AD)-crosslinked casein films: synthesis, characterization and water absorption behavior. *Designed Monomers and Polymers*, 19(5), 406-419.
26. El-Houssiny, A.S.; Ward, A.A; Mostafa, D.M.; Abd-El-Messieh, S.L.; Abdel-Nour, K.N.; Darwish, M.M.; and Khalil, W.A. (2016). Drug-polymer interaction between glucosamine sulfate and alginate nanoparticles: FTIR, DSC and dielectric spectroscopy studies. *Advances in Natural Sciences: Nanoscience and Nanotechnology*, 7(2), 025014.
27. Girsova, M.A.; Golovina, G.F.; Anfimova, I.N.; Arsent'ev, M.Y.; and Antropova, T.V. (2016). Structure and spectral properties of the silver-containing high-silica glasses. *Journal of Physics Conference Series*, 741(1), 012144.
28. Sharma, C.; Dinda, A.K.; Potdar, P.D.; Chou, C.F.; and Mishra, N.C. (2016). Fabrication and characterization of novel nano-biocomposite scaffold of chitosan-gelatin-alginate-hydroxyapatite for bone tissue engineering. *Materials Science and Engineering: C*, 64, 416-427.
29. Kavya, K.C.; Jayakumar, R.; Nair, S.; and Chennazhi, K.P. (2013). Fabrication and characterization of chitosan/gelatin/nSiO2 composite scaffold for bone tissue engineering. *International Journal of Biological Macromolecules*, 59, 255-263.
30. Maji, K.; Dasgupta, S.; Pramanik, K.; and Bissoyi, A. (2016) Preparation and evaluation of gelatin-chitosan-nanobioglass 3D porous scaffold for bone tissue engineering. *International Journal of Biomaterials*, 2016, 9825659.